Chapter – V
Effect of 140 MeV Ag^{11+} Ions on Polymer Composites

Abstract

In this chapter swift heavy ion (140MeV, Ag^{11+} ions) induced modification of Ferric oxalate and Pd(acac) dispersed PMMA films at the fluences of $1x10^{11}$ and $5x10^{12}$ ions/cm^2 were studied. This study has been carried out to support the results obtained in chapter 4. Dielectric properties shows significant enhancement after Ag^{11+} irradiation. XRD analysis of PMMA+Pd(acac) reveals the decrease in crystalline size and % crystallinity after SHI irradiation. AFM result shows that average surface roughness increases after irradiation. Overall, this chapter represent supportive data for the results of Chapter-4 on the effect of SHI irradiation.

5.0 Introduction

The effect of ion beam has already been carried out using proton and Ni^{10+} beam and is discussed in Chapter 3 and 4 respectively. Keeping more pronounced effect of SHI (than that of light ion) on the material in consideration, further study was extended to determine SHI effect on polymer composites using 140 MeV Ag^{11+} ions on two of the composites studied previously using proton and Ni^{10+} ion beams.

This chapter deals with the effect of SHI irradiation on following polymer composites.

(i) PMMA+Fo

(ii) PMMA+Pd(acac)

Properties and preparation method of composites have been discussed in Chapter-2. The films were irradiated with 140 MeV Ag^{11+} ions at the fluences of $1x10^{11}$ and $5x10^{12}$ ions/cm^2 from the Pelletron of the Inter University Accelerator Centre (IUAC), New Delhi. AC electrical, structural, chemical properties and surface morphology of the composites were carried out to ensure the effect of SHI on organometallic compound dispersed polymer composites.

5.1 Effect of SHI (140 MeV Ag^{11+}) on PMMA+Fo composites

5.1.1 AC electrical properties

(i) AC electrical Conductivity

The ac conductivity of the pristine and irradiated composite films was calculated using equation 2.3.13 (section 2.3) of Chapter-2. Figure 5.1 (a-d) shows the conductivity as a function of the frequency and fluence. Figure 5.1 (e) shows variation

in conductivity with filler concentration. The AC conductivity of the composites increases with increasing frequency, filler concentration and also with ion fluence.

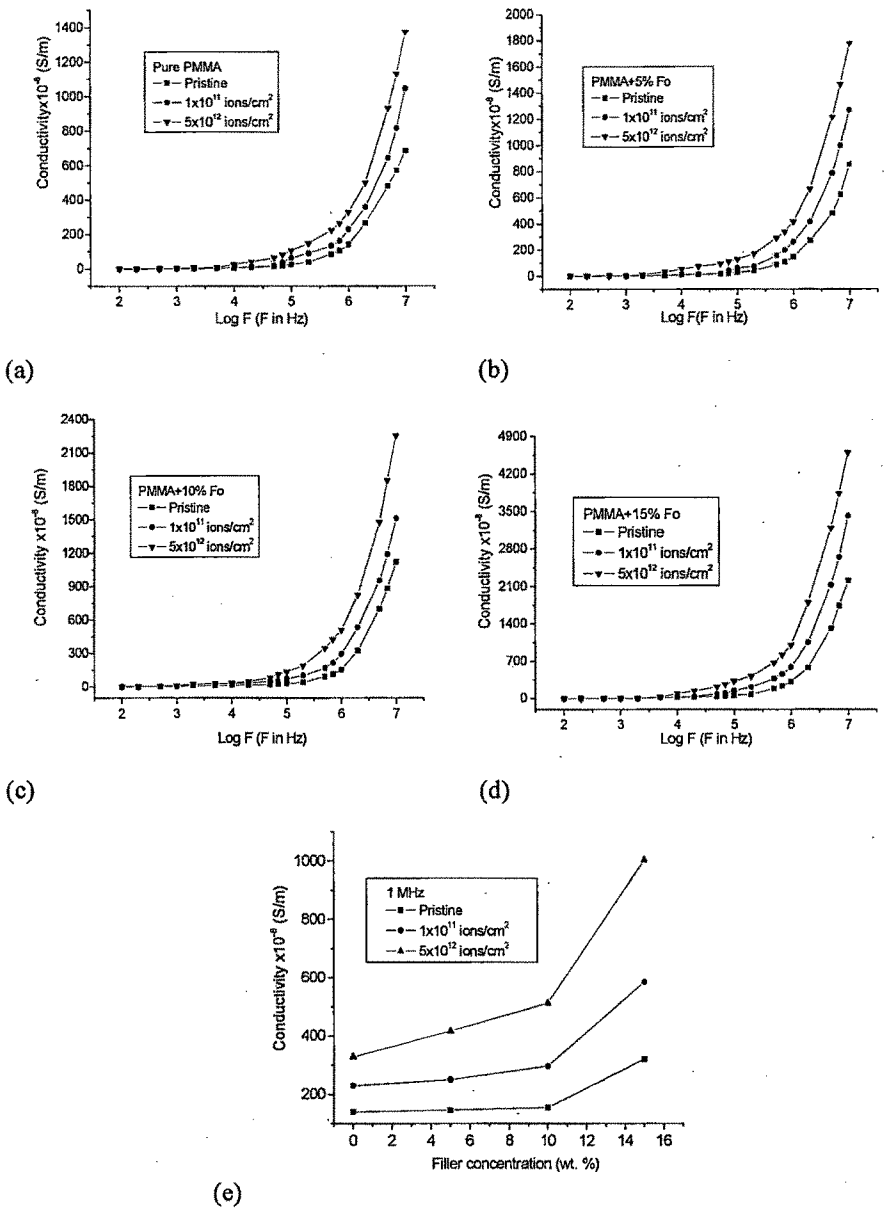

Fig. 5.1 AC conductivity versus log frequency of pristine and irradiated films of (a) Pure PMMA, (b) PMMA+5%Fo, (c) PMMA+10%Fo and (d) PMMA+15%Fo (e) Variation of AC conductivity with filler concentration at 1 MHz

Generally electrical conducting path and network of connection could be formed in the composites with increasing the content of the filler. Irradiation further promotes the metal to polymer bonding and convert the polymeric structure to a hydrogen depleted carbon network, which makes the polymers more conductive [1, 2]. Similar results are also explained in Chapter-4.

(ii) Dielectric property

Dielectric constant of all samples was determined using equation 2.3.15 (Chapter-2). Fig. 5.2(a-d) shows the variation of dielectric constant of pristine and irradiated PMMA/Fo composites as a function of frequency and fluence. Fig. 5.2 (e) shows variation in dielectric constant with filler concentration.

For pristine and irradiated composite films, the dielectric constant remains almost constant up to 100 kHz and decreases at higher frequencies and obey the Universal law [3] of dielectric constant i.e. $\varepsilon \alpha f^{n-1}$, where n is the power law exponent and varies between zero to one. It is observed that n decreases as concentration increases and increases as fluence increases. Similar results were also obtained in case of proton and Ni^{10+} irradiations.

The increase in the dielectric constant with filler content is a direct consequence of interfacial polarization effect between polymer and the filler particles [4]. The quantity of the accumulated charges will increase in the composite after doping because of the polarization of the PMMA/filler at the interfaces. The polarization makes an additional contribution to the charge quantity. It is observed that the dielectric constant increases on increasing the concentration of filler as shown in Fig. 5.2 (e).

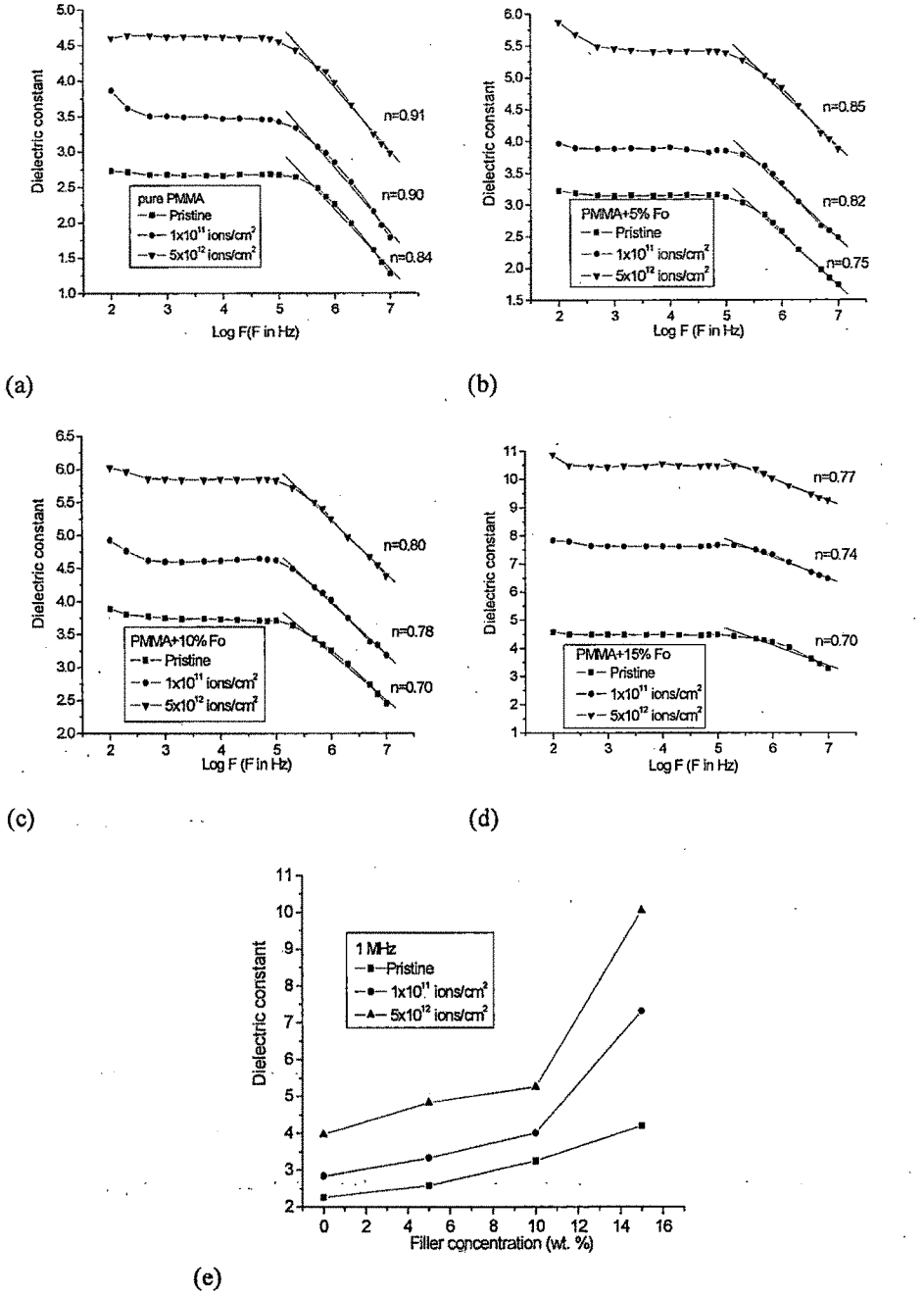

Fig. 5.2 Dielectric constant versus log frequency for pristine and irradiated films of (a) Pure PMMA, (b) PMMA+5%Fo, (c) PMMA+10%Fo and (d) PMMA+15%Fo films (e) Variation of AC conductivity with filler concentration at 1 MHz

The dependence of dielectric loss on frequency and fluence is plotted in Fig. 5.3 (a-d). The loss factor (tanδ) shows strong frequency dependence and it decreases exponentially as frequency increases. The positive value of dielectric loss shows the inductive behaviour of the sample.

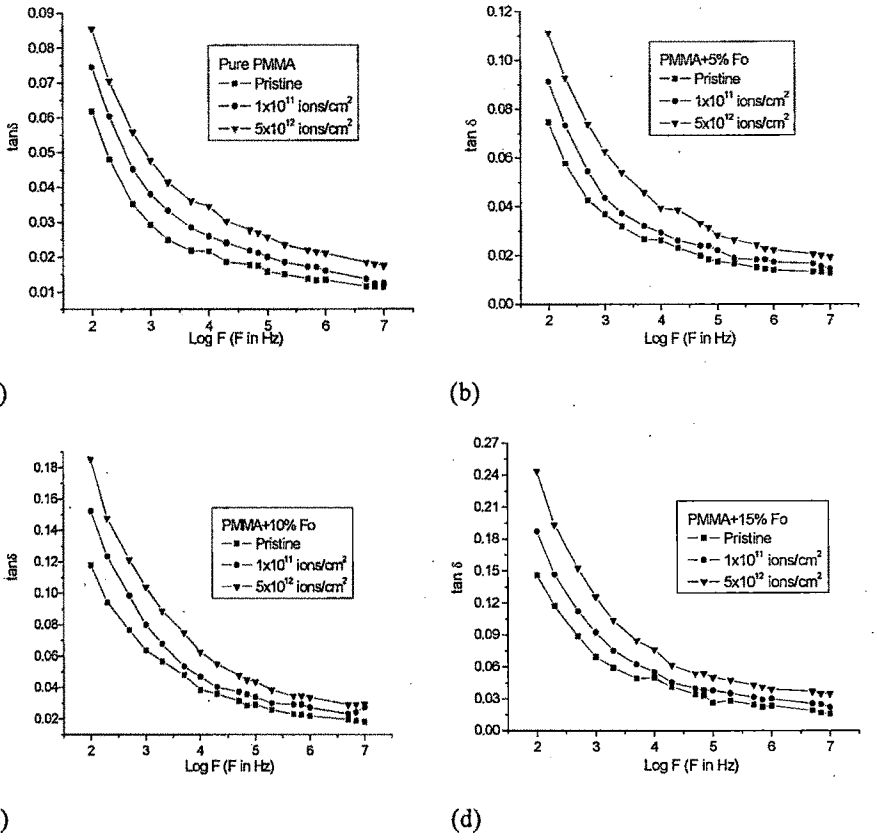

Fig. 5.3 Dielectric loss versus log frequency for pristine and irradiated films of (a) Pure PMMA, (b) PMMA+5%Fo, (c) PMMA+10%Fo and (d) PMMA+15%Fo films

5.1.2 FTIR analysis

Figure 5.4(a) and (b) show the FTIR spectra of the pristine and irradiated (at fluence of $5x10^{12}$ ions/cm^2) samples respectively, for different filler concentrations. The presence of different functional groups in the structure has been identified as (a) 750

and 810 cm^{-1} ; CH_2 rocking vibration (b) 700-1500 cm^{-1}; C-O stretching vibration (c) 1350-1450 cm^{-1} ; C-H bending vibration (d) 1730 cm^{-1}; C=O stretching vibrations in the pendant group (-$COOCH_3$) of PMMA (e) 2010 cm^{-1} ;C=C stretching vibration [5].

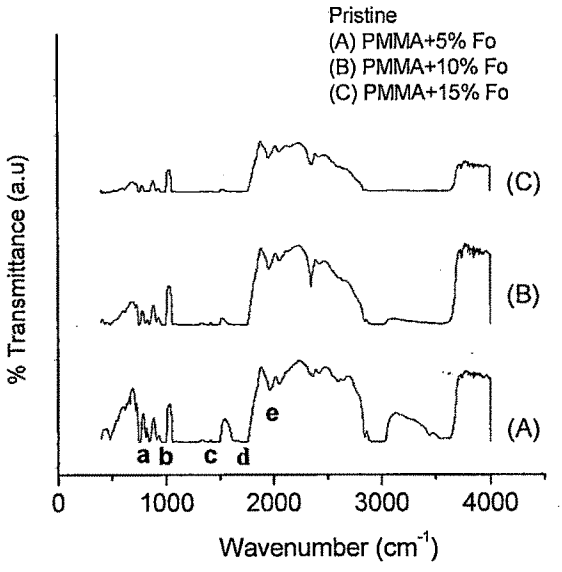

(a)

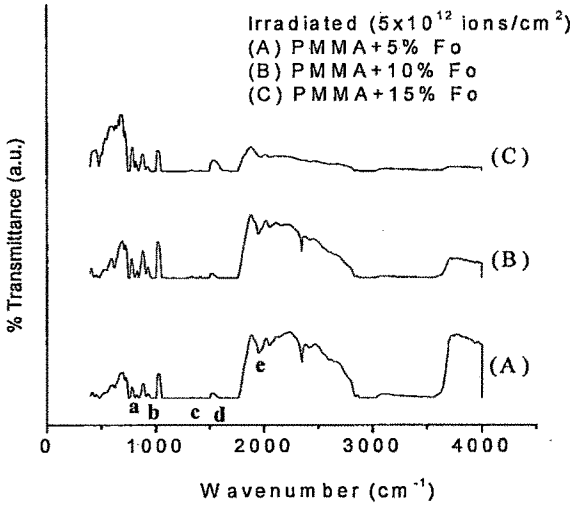

(b)

Figure 5.4 FTIR spectra of (a) Pristine and (b) Irradiated ($5x10^{12}$ ions/cm^2) films

The absorption peaks at higher wavenumber decrease sharply as filler concentration increases. It might be due to formation of bond of organometallic compound with polymeric chains by breaking traditional polymeric bond. Significant reduction in peak intensity was observed after SHI irradiation. This might be attributed to breakage of the C-O, C=O bonds and CH_2, CH_3 groups due to large energy deposition in the sample due to SHI irradiation [6-8] as also explained in Chapter-4.

5.1.3 Atomic force microscopy

The surface morphology of pristine and irradiated films of 5%, 10% and 15% Fo dispersed PMMA was studied by AFM on 2×2 μm^2 area as shown in Fig. 5.5 (a-f). Each AFM image was analysed in terms of average surface roughness (Ra). The average roughness obtained for pristine samples are 4.7, 7.7 and 24.1 nm for 5, 10 and 15% Fo dispersed PMMA samples respectively. The roughness values of correspondingly irradiated (at a fluence of $5x10^{12}$ ions/cm^2) samples are 8.0, 17.5 and 48.2 nm respectively. It is found that roughness increases as ferric oxalate concentration increases and also after irradiation. SHI irradiation leads to large sputtering effects on polymeric surface. Increase in filler concentration leads to increase of density and size of metal particles on the surface of PMMA film which is responsible for increase in average surface roughness with filler concentration [9]. Similar results are also obtained in previous chapter for the same composite.

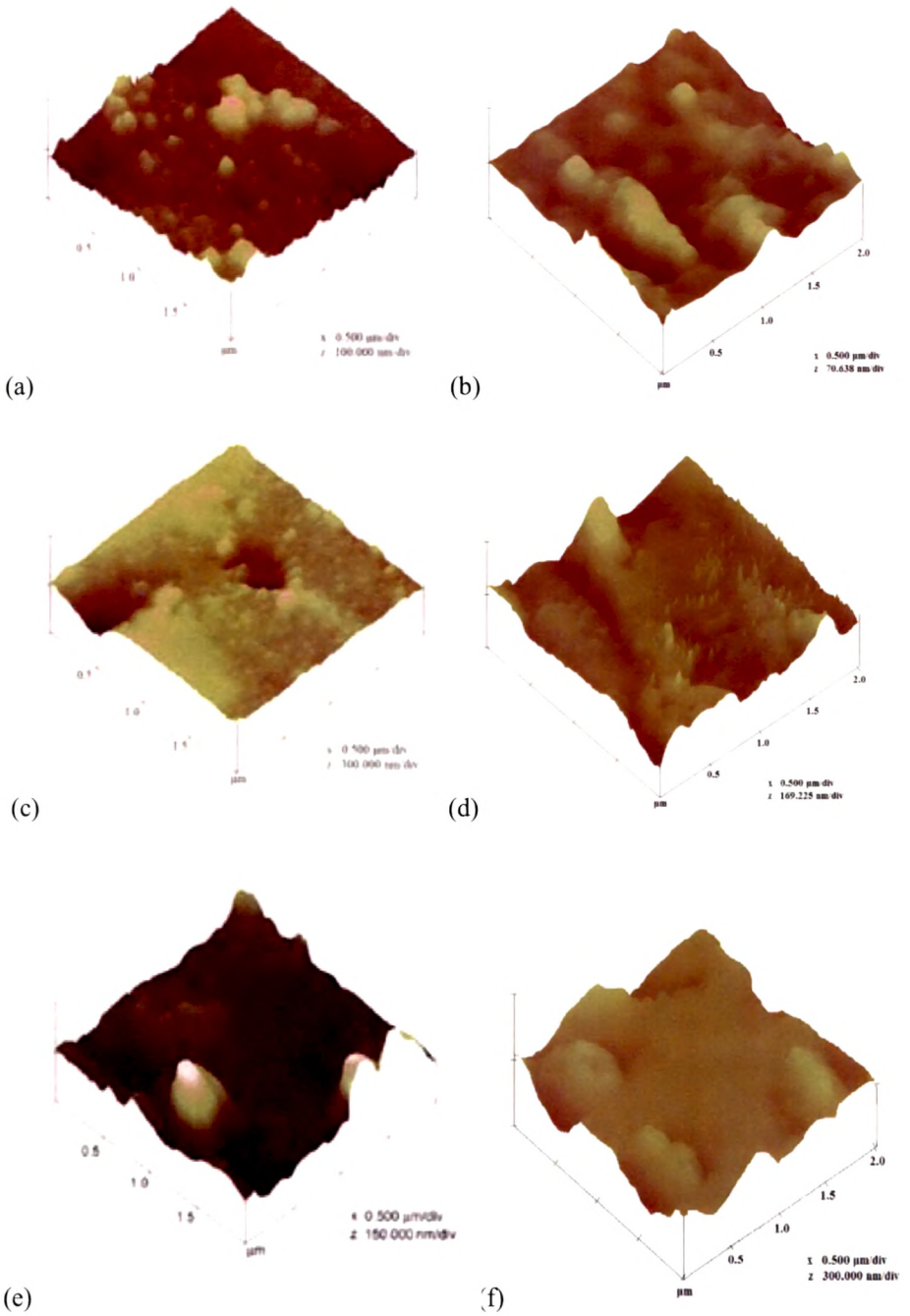

Fig. 5.5 AFM images of (a) PMMA+5% Fo (pristine) (b) PMMA+5% Fo (irradiated) (c) PMMA+10% Fo (pristine) (d) PMMA+10% Fo (irradiated) (e) PMMA+15% Fo (pristine) (f) PMMA+15% Fo (irradiated)

5.1.4 Conclusion

AC electrical properties of pristine and irradiated organometallic compound dispersed PMMA films were investigated. Ion irradiation significantly enhanced dielectric properties of the composites. The dielectric constant remains constant up to 100 kHz and then decreases slowly with increasing frequency and increases gradually with the increase of the concentration of filler. Dielectric loss/constant is observed to change significantly due to irradiation. Thus AC electric properties of the composites show frequency, filler and fluence dependent behaviour. FTIR results reveal that there is decrease in peak intensity of some polymeric bonds due to the emission of hydrogen and/or other volatile gases upon irradiation. The surface roughness increases as ferric oxalate concentration increases and also with the fluence as observed from AFM studies. Similar results were also obtained for Ni^{10+} irradiated samples.

5.2 Effect of SHI on PMMA+Pd(acac) composites

5.2.1 AC electrical properties

(i) AC electrical Conductivity

The ac conductivity of the pristine and irradiated composite films was calculated using equation 2.3.13 (section 2.3) of Chapter-2. Fig. 5.6 (a-d) shows the conductivity as a function of the frequency and fluence. Fig. 5.6 (e) shows variation in conductivity with filler concentration. AC conductivity increases with filler concentration. Conductive nature of filler is responsible for forming conductive phase in polymer matrix and increase in conductivity. Further enhancement in conductivity was obtained upon irradiation, which is attributed to emission of the hydrogen and/or other volatile gases from the matrix due to large energy deposition by SHI irradiation [1]. 120 MeV Ni^{10+} ion irradiation also showed similar effect on these composites [2].

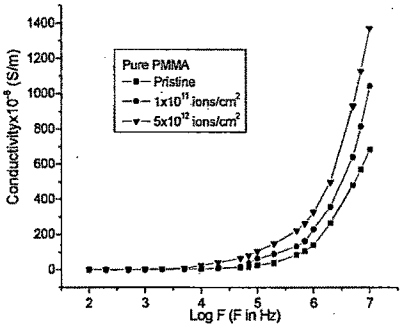

(a)

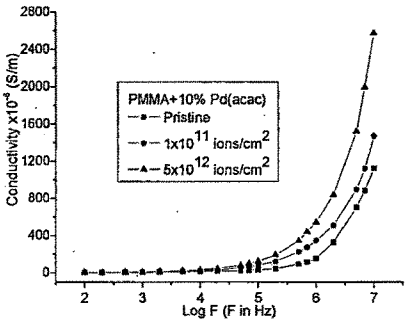

(b)

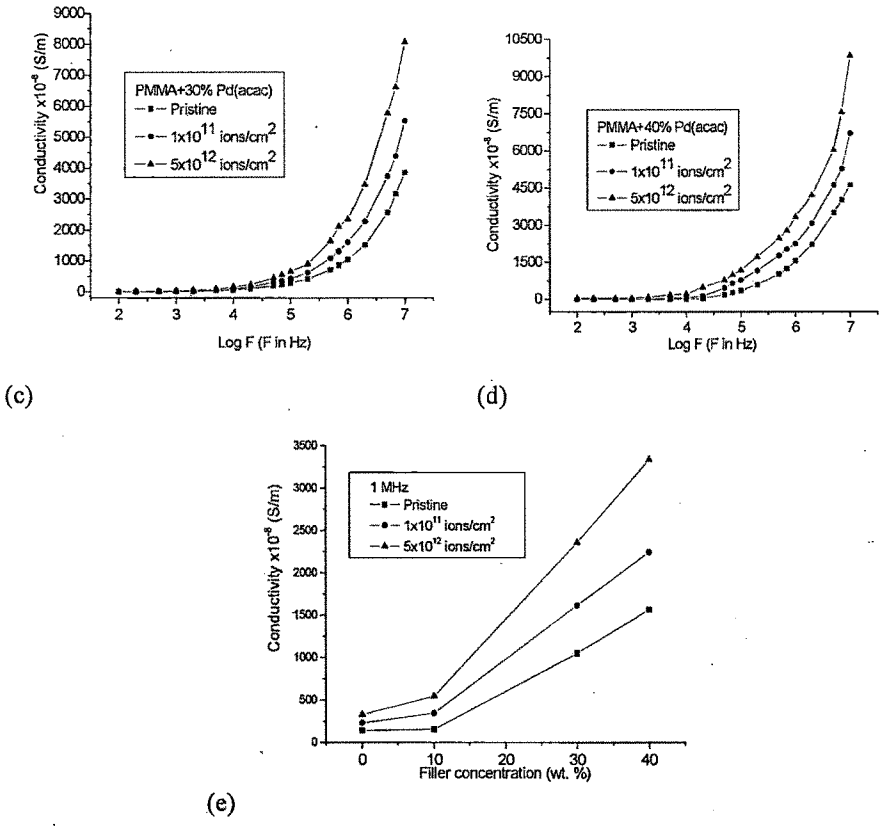

Fig. 5.6 AC conductivity versus log frequency of pristine and irradiated films of (a) Pure PMMA, (b) PMMA+10% Pd(acac), (c) PMMA+30% Pd(acac) and (d) PMMA+40% Pd(acac) films (e) Variation of AC conductivity with filler concentration at 1 MHz

(ii) Dielectric Properties

Dielectric constant of all samples was determined using equation 2.3.15 (Chapter-2). Fig. 5.7(a-d) shows the variation of dielectric constant of pristine and irradiated PMMA+Pd(acac) composites as a function of frequency and fluence. Fig. 5.7(e) shows variation in dielectric constant with filler concentration. For pristine and irradiated composite films, the dielectric constant remains almost constant up to 100 kHz and decreases at higher frequencies. In all cases it follows Universal law of dielectric i.e. $\varepsilon \alpha f^{n-1}$ where $0<n<1$ [3].

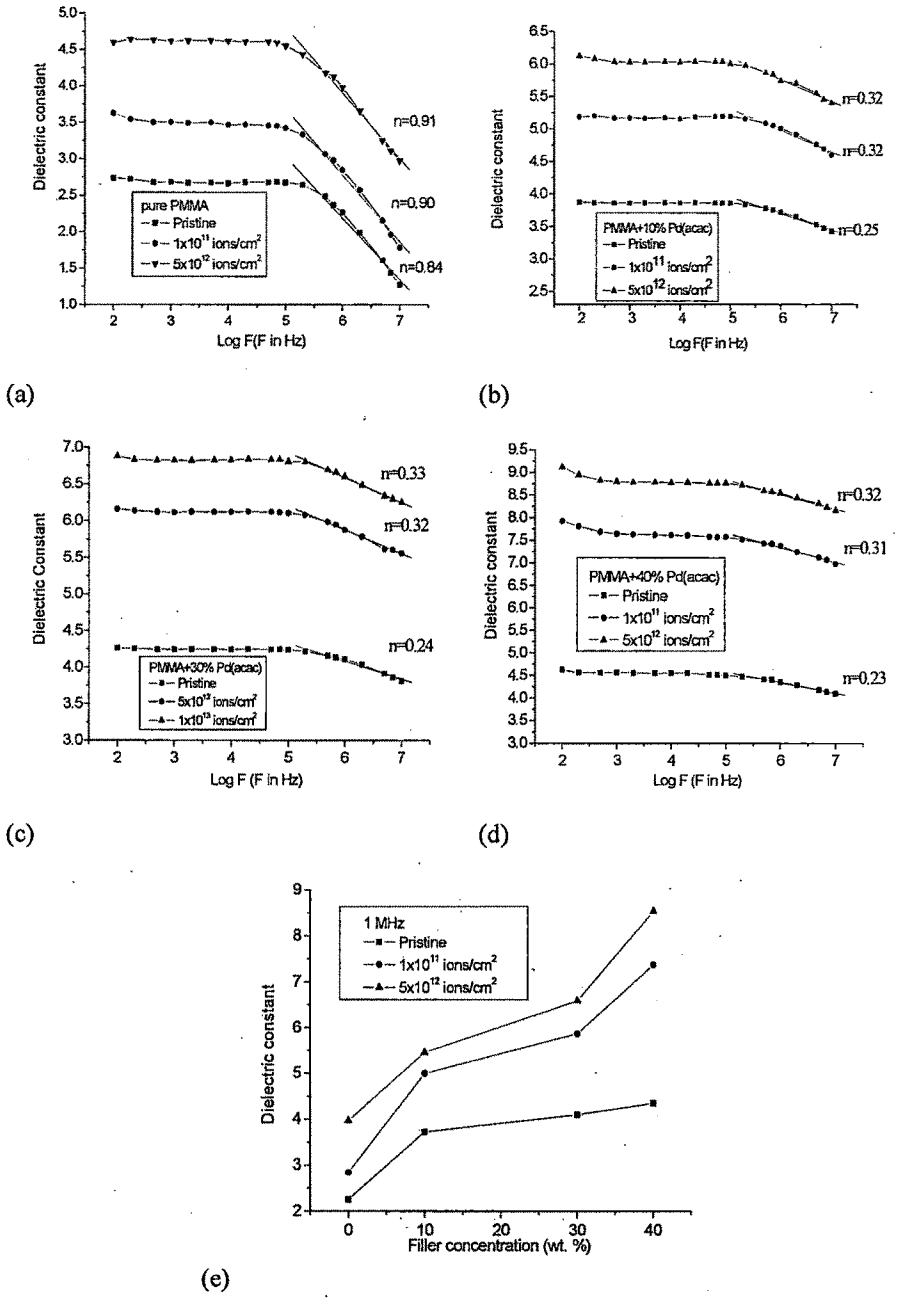

Fig. 5.7 Dielectric constant versus log frequency for pristine and irradiated films of (a) Pure PMMA, (b) PMMA+10% Pd(acac), (c) PMMA+30% Pd(acac) and (d) PMMA+40% Pd(acac) films (e) Variation of AC conductivity with filler concentration at 1 MHz

Due to dispersion of organometallic compound, the quantity of the accumulated charges will increase because of the polarization of the polymer/metal at interfaces. The polarization makes an additional contribution to the charge quantity. Therefore the dielectric constant of the composites will be higher than the pure polymer [10, 11].

According to Dissado and Hill theory at high frequency, intra-cluster motions are dominant. In intra-cluster motions, the relaxation of a dipole will produce a 'chain' response in its neighbouring dipoles and the reaction of the neighbouring dipoles will, in turn, affect the first dipole, so the overall effect will be seen as a single cluster dipole moment relaxation [9]. This reduces the dielectric constant at higher frequencies [2]. It is also observed that the dielectric constant increases with increasing the concentration of filler as shown in Fig. 5.7 (e).

The dependence of dielectric loss on frequency and fluence has been plotted in Fig. 5.8 (a-d). Dielectric loss increases with filler concentration and also upon irradiation. However, it decreases at high frequency which reveals that as frequency increases, the induced charges gradually fail to follow the reversing field causing reduction in electronic oscillation.

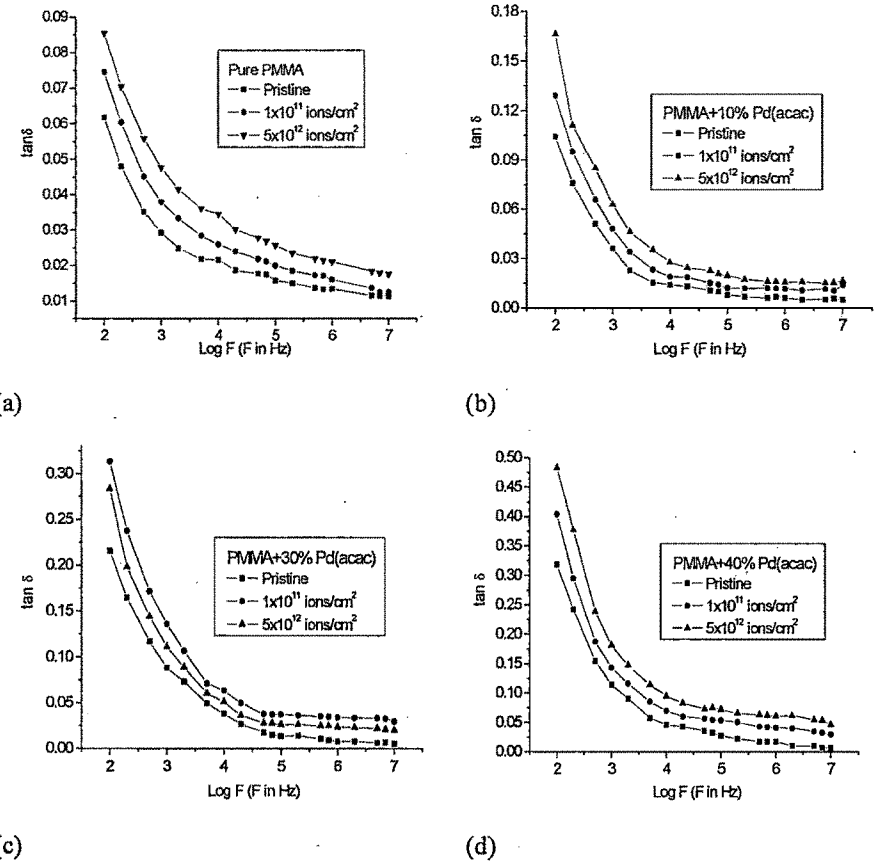

Fig. 5.8 Dielectric loss versus log frequency for pristine and irradiated films of (a) Pure PMMA, (b) PMMA+10% Pd(acac), (c) PMMA+30% Pd(acac) and (d) PMMA+40% Pd(acac) films

5.2.2 X-ray diffraction (XRD)

Fig. 5.9 (a-c) represents the diffraction patterns of the pristine and irradiated samples for the most prominent peaks. The nature of the peak indicates the semi-crystalline nature of the sample. In both the cases, (i.e. the pristine and irradiated films) the peaks obtained at the same position but with the different intensity.

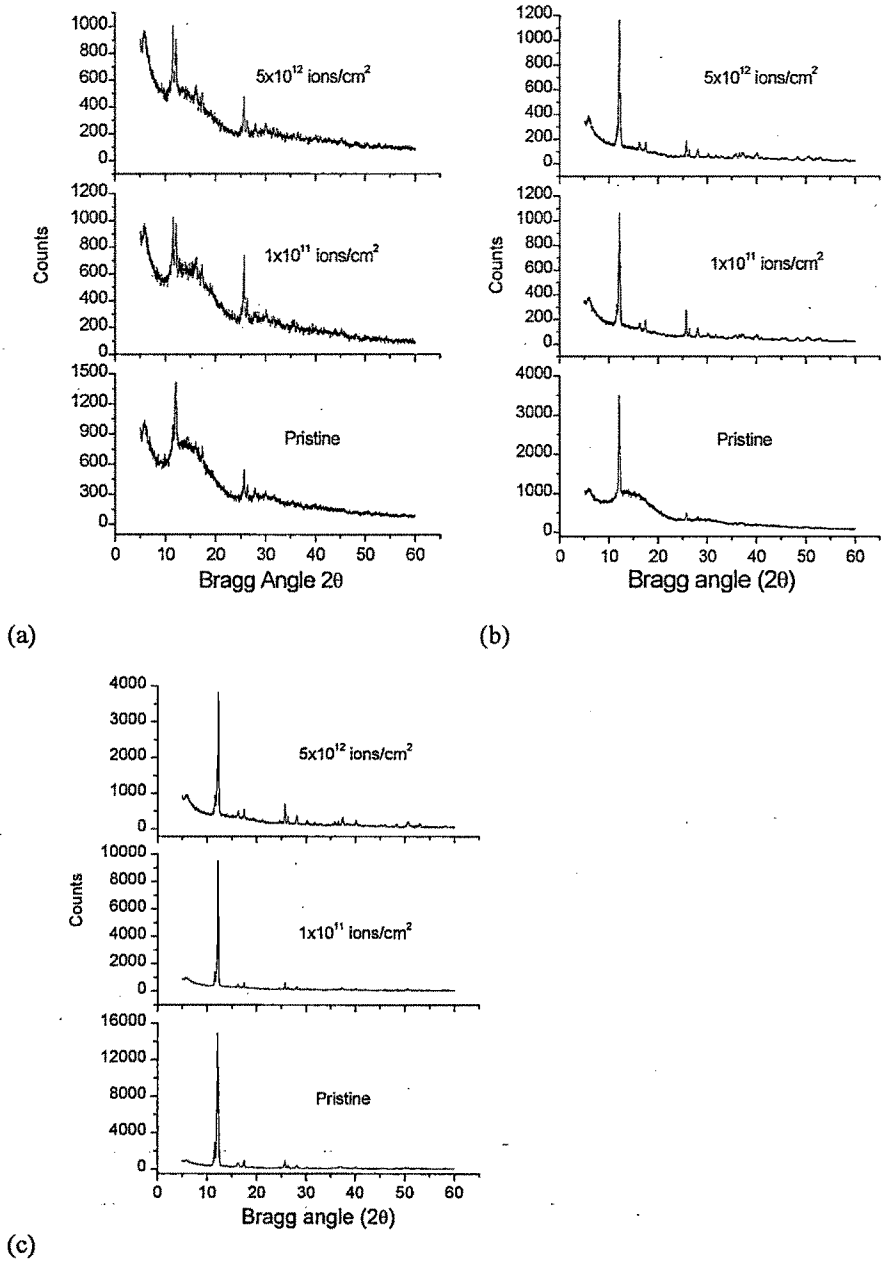

Fig. 5.9 XRD spectrum of Pristine and irradiated composites of (a) PMMA+10% Pd(acac), (b) PMMA+30% Pd(acac) and (c) PMMA+40% Pd(acac)

The crystallite size has been calculated before and after the irradiation using Scherrer's equation [13].

$$D = \frac{K\lambda}{l\cos\theta}$$

where K is constant approximately equal to unity and related to the crystalline shape, l is FWHM of the diffraction peak, D is crystalline size and θ is the angle between the atomic plane and both the incident and reflected beams.

The crystallite size obtained using above equation is listed in Table 5.1.

Table 5.1 Cryastalline size and % Crystallinity measurement

Sample	Crystalline size (nm)			% Crystallinity		
	Pristine	$1x10^{11}$ ions/cm^2	$5x10^{12}$ ion/cm^2	Pristine	$1x10^{11}$ ions/cm^2	$5x10^{12}$ ion/cm^2
PMMA+10% Pd(acac)	6.6	5.4	4.6	10.2	6.8	7.1
PMMA+30% Pd(acac)	22.7	21.2	16.9	17.3	11.9	11.6
PMMA+40% Pd(acac)	23.4	21.2	19.7	38.8	22.0	13.5

It is apparent that the crystalline size and % crystallinity increases with filler concentration which is responsible to the crystalline nature of filler. But it reduces after irradiation, which is attributed to splitting of crystalline grains due to large energy deposition by SHI irradiation [14, 15]. Similar results are also obtained by using 120 MeV Ni^{10+} ion irradiated films.

5.2.3 FTIR Spectroscopy

FTIR spectra of pristine and irradiated films of 10, 30, 40% Pd(acac) doped films have been studied and plotted in Fig. 5.10 (a,b).

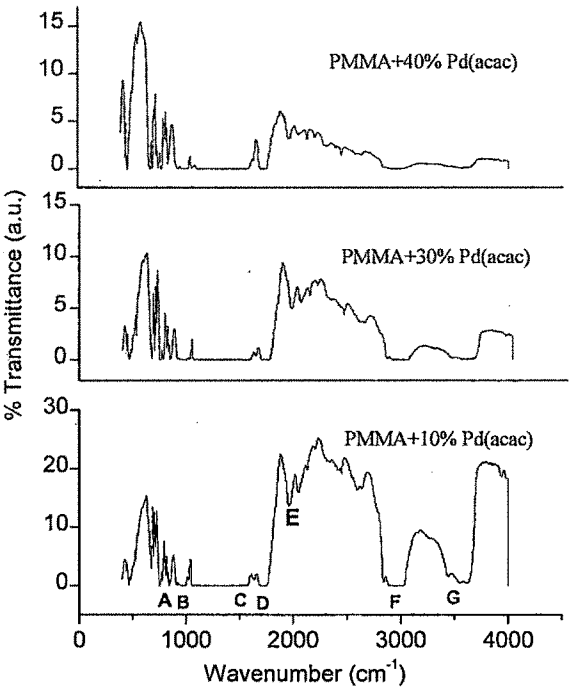

(a)

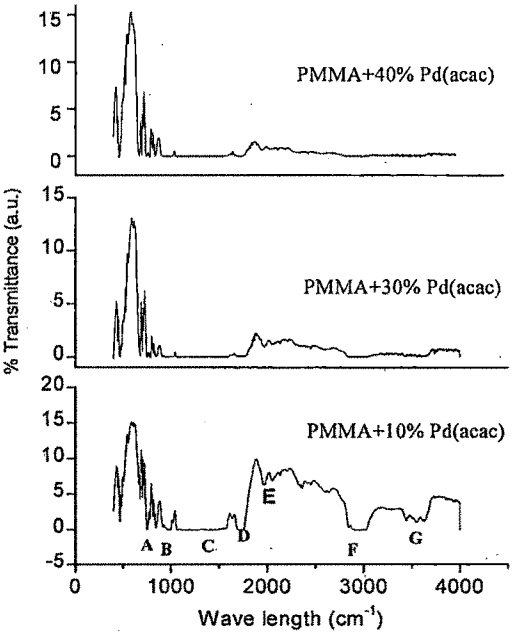

(b)

Fig. 5.10 FTIR spectrum for (a) Pristine and (b) Irradiated ($5x10^{12}$ ions/cm^2) composite films

The absorption bands are identified as (a) CH_2 rocking vibration (751 cm^{-1}), (b) CH_3 rocking (847 cm^{-1}), (c) C-O stretching vibration (990-1270 cm^{-1}), (d) C=O stretching vibration (1600-1800 cm^{-1}) (e) C=C stretching vibration (1920-2100 cm^{-1}) (f) C-H stretching vibration of CH_2 and CH_3 (2820–3080 cm^{-1}) (g) OH free stretching vibration (3400- 3600 cm^{-1}) [5]. The C-O and C=O groups show a strong absorption in the range (990-1200 cm^{-1}) and (1600-1800 cm^{-1}) respectively depending on the immediate environment of these groups. However, after irradiation, the peak intensities of functional groups are reduced due to emission of hydrogen and/or other volatile gases (Fig. 5.10(b)). This may be attributed to the breakage of chemical bonds and formation of free radicals, unsaturation, etc as explained in Chapter-4.

5.2.4 Atomic force microscopy (AFM)

Surface morphology of pristine and irradiated composites was studied using atomic force microscopy in contact mode with silicon nitride (Si_3N_4) tip at IUC, Indore. The 3-dimension morphology of pristine and Ag^{11+} irradiated (at a fluence of $5x10^{12}$ ions/cm^2) samples of 10 and 30% Pd(acac) doped PMMA are shown in Fig 5.11(a,b) and Fig. 5.11(c, d) in 2x2 μm^2 area respectively.

Average surface roughness was observed 7.6 nm for PMMA+10% Pd(acac) and 11.4 nm for PMMA+30% Pd(acac) and it increases to 9.4 nm and 16.0 nm respectively after irradiation. The increase in roughness with concentration of filler is ascribed to increase in density and size of metal particles on the surface of the polymer matrix. The roughness further increases after irradiation which might be due to large sputtering effect [6, 11, 16].

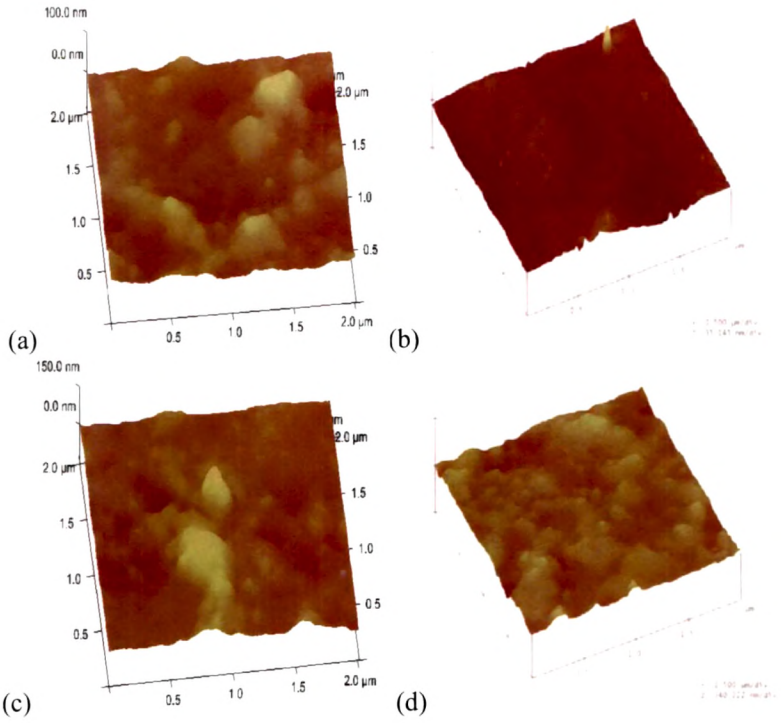

Fig. 5.11 AFM images of (a) PMMA+10% Pd(acac)-Pristine (b) PMMA+10% Pd(acac)-Irradiated (c) PMMA+30% Pd(acac)-Pristine and (b) PMMA+30% Pd(acac)-Irradiated

5.2.5 Conclusions

Dispersion of organometallic compound [Pd(acac)] in PMMA films enhanced the dielectric properties of pure polymer significantly. Dielectric properties are further enhanced by SHI irradiation. This may be attributed to the hydrogen depleted carbon network formed due to removal of hydrogen and/or other volatile gases from the polymer matrix. An XRD analysis reveals that the crystalline size of the organometallic compound has decreased after Ag^{11+} irradiation. Crystallinity of the composites decreases after irradiation due to chain scissioning which induces amorphization. FTIR results also support scissioning effect. The peak intensity of various functional groups is observed to decrease after irradiation. AFM images explain the increase in average surface roughness after irradiation. In general, Ag^{11+} irradiated sample shows similar behaviour as Ni^{10+} irradiated samples.

5.3 Summary

Two different composites have been studied using 140 MeV Ag^{11+} ions irradiation. AC electrical, structural and surface properties have been studied using different characterization techniques.

AC electrical conductivity of all pristine and irradiated composites for 10% filler concentration at 10 MHz frequency. is shown in Fig. 5.12.

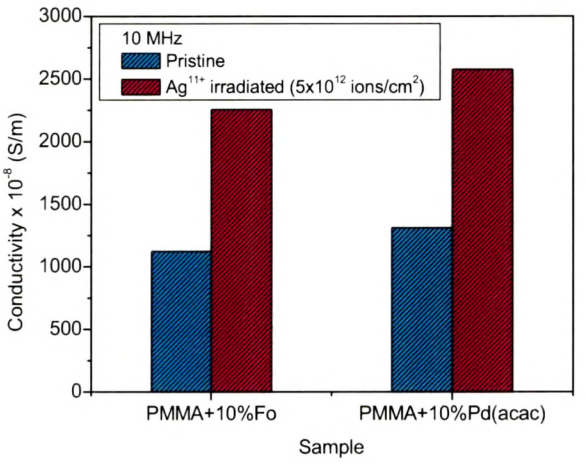

Fig. 5.12 Comparison of conductivity of pristine and irradiated ($5x10^{12}$ ions/cm^2) composites at 10 MHz frequency for different filler in PMMA

Conductivity is observed to increase after irradiation. Electrical conductivity depends on the types of filler. The result shows that the conductivity is higher for Pd(acac) than Fo for same concentration of filler. Ion beam irradiation further improves AC electrical conductivity due to conversion of the polymeric structure in to a hydrogen depleted carbon network.

Similar study for dielectric constant of all composites have been done and shown in Fig. 5.13. It is observed that the dielectric constant increases after irradiation.

Dielectric loss was studied for all pristine and irradiated composites and results show frequency and fluence dependent behaviour for all cases.

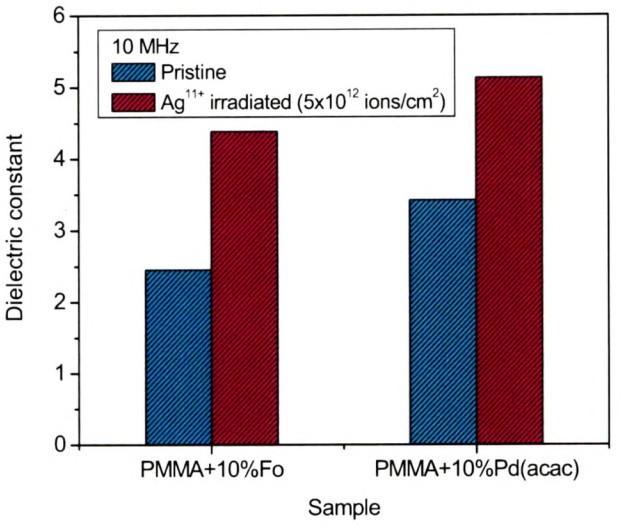

Fig. 5.13 Comparison of dielectric constant of pristine and irradiated ($5x10^{12}$ ions/cm^2) composites at 10 MHz frequency for different filler in PMMA

XRD patterns of pristine and irradiated samples of PMMA+Pd(acac) have been studied and the results reveal that the crystalline size and %crystallinity of the sample decreased upon irradiation.

FTIR images show small shift and alteration in the peak position due to changes in the nearest surrounding of the functional groups because of the presence of filler particles and also after irradiation.

AFM study reveals that the average surface roughness increases after irradiation in all cases due to large sputtering effect because of SHI interaction with composite. All results are corroborated with the results obtained using Ni^{10+} ions as discussed in Chapter-4.

Reference

[1] Y.Q.Wang, M. Curry, E. Tavenner, N. Dobson, R.E. Giedd. Nucl Instrum Meth. B 219-220 (2004) 798.

[2] N.L.Singh, Sejal Shah, Anjum Qureshi, F. Singh, D.K.Avasthi, V.Shrinet, V.Ganesan Poly. Degrad. Stab. 93 (2008) 1088.

[3] A.K. Jonscher. Nature 267(1977) 673.

[4] S. Ghany, A.E. Salam, G. M. Nasr. J Appl Polym Sci. 77 (2000) 1816.

[5] H.W.Choi, H.J.Woo, W.Hong, J.K.Kim, S.K.Lee, C.H.Eum. Appl. Surf. Sci 169 (2001) 433.

[6] X. Yan, X. Tao, X. Shan, W. Xiaobo, Y. Shengrong. Nanotechnology 15 (2004) 1759.

[7] D.M. Ruck, J. Schulz, N. Deusch, Nucl. Instrum. Meth B 131 (1997) 149.

[8] L. Calcagno, Nucl. Instrum. Meth B 105 (1995) 63.

[9] N. L. Singh, A. Qureshi, F. Singh, D. K. Avasthi Mat. Sci and Eng. A 547 (2007) 195.

[10] Z. M. Dang, Y.H. Zhang, S-C. Tjong. Synth Met 146 (2004) 79.

[11] N.L.Singh, Sejal Shah, Anjum Qureshi, P. K. Kulariya, D. K. Avasthi, A. M. Awasthi. Rad. Eff. and Def. in Solids 164 (10) (2009) 619.

[12] A. Pelaiz-Barranco, Scripta Materialia 54 (2006) 47.

[13] P. Scherrer, Gott. Nachar 2 (1918) 98.

[14] H.S. Virk, P.S.Chandi and A.K. Srivastava, Bull. Mater. Sci. 24(5) (2001) 529.

[15] V. Singh, T. Singh, A. Chandra, S. K. Bandyopadhyay, P. Sen, K. Witte, U. W. Scherer, A. Srivastava, Nucl. Instrum. Meth B 244 (2006) 243.

[16] L. Singh, K. S. Samra, Nucl. Instrum Meth B 263 (2007) 458.